A mutant herpes simplex virus type 1 thymidine kinase reporter gene shows improved sensitivity for imaging reporter gene expression with positron emission tomography

Sanjiv S. Gambhir*[†‡§¶‖], Eileen Bauer*[†], Margaret E. Black**[,††], Qianwa Liang*[†,‡‡], Mark S. Kokoris**, Jorge R. Barrio[†‡], Meera Iyer*[†], Mohammad Namavari[†‡], Michael E. Phelps*[†‡§], and Harvey R. Herschman*[†‡¶‡‡]

*The Crump Institute for Biological Imaging, †University of California/Department of Energy Laboratory of Structural Biology and Molecular Medicine, and ‡Department of Molecular and Medical Pharmacology, Division of Nuclear Medicine, ‡‡Molecular Biology Institute, §Department of Biomathematics, and ¶University of California–Jonsson Comprehensive Cancer Center, University of California School of Medicine, Los Angeles, CA 90095-1770; and **Chiroscience R & D, Inc., Bothell, WA 98021; and ††Department of Pharmaceutical Sciences, Washington State University, Pullman, WA 99164

We are developing assays for noninvasive, quantitative imaging of reporter genes with positron emission tomography (PET), for application both in animal models and in human gene therapy. We report here a method to improve the detection of lower levels of PET reporter gene expression by utilizing a *mutant* herpes simplex virus type 1 thymidine kinase (HSV1-sr39tk) as a PET reporter gene. The HSV1-sr39tk mutant was identified from a library of site-directed mutants. Accumulation (net uptake) of the radioactively labeled substrates [8-³H]penciclovir ([8-³H]PCV), and 8-[¹⁸F]fluoropenciclovir (FPCV) in C6 rat glioma cells expressing HSV1-sr39tk is increased by a factor of ≈2.0 when compared with C6 cells expressing wild-type HSV1-tk. The increased imaging sensitivity of HSV1-sr39tk when FPCV is used is also demonstrated *in vivo* both with tumor cells stably transfected with either HSV1-tk or HSV1-sr39tk, and after hepatic delivery of HSV1-tk or HSV1-sr39tk by using adenoviral vectors. The use of HSV1-sr39tk as a PET reporter gene and FPCV as a PET reporter probe results in significantly enhanced sensitivity for imaging reporter gene expression *in vivo*.

Several approaches are being developed to image reporter gene expression in living animals. These include methods that rely on charge-coupled device camera imaging and bioluminescent reporter genes (1), single-photon emission computed tomography using the herpes simplex virus type 1 thymidine kinase (HSV1-tk) reporter gene (2), approaches that use magnetic resonance imaging (reviewed in ref. 3), methods based on the HSV1-tk reporter gene and positron emission tomography (PET) (4, 5), and the use of the dopamine type 2 receptor (D2R) as a reporter gene for PET (6). The use of reporter genes that can be imaged *in vivo* will permit many different applications, including monitoring of both somatic gene transfer and transgenic/knock-in reporter gene expression (7).

PET provides repeated, noninvasive imaging of biological processes in living subjects (8, 9). PET utilizes molecular probes labeled with positron-emitting radioisotopes (e.g., fluorine-18, with a half-life of 110 min). PET probes typically are either positron-labeled ligands for receptors or positron-labeled substrates for intracellular enzymes. Tracer quantities of PET probes yield a tomographic image after their retention, as a consequence of either binding of positron-labeled ligand to a receptor or conversion of positron-labeled substrate to "trapped" metabolic product(s). PET is particularly well suited for application to human studies. PET reporter gene imaging in humans will allow monitoring of the location(s), magnitude, and duration of therapeutic/suicide gene expression, by using vectors for DNA delivery in which the reporter gene and therapeutic gene are expressed from a common transcript (10, 11). To noninvasively image biological processes in small animals such as

mice, we have recently developed microPET technology with a volumetric resolution of approximately (2 mm)³ (12).

HSV1-tk is under active study as a reporter gene to image gene expression in living individuals (reviewed in ref. 11). (Note: HSV1-tk refers to the gene, HSV1-TK refers to the enzyme.) HSV1-TK phosphorylates a range of substrates, including acycloguanosines (e.g., acyclovir, ganciclovir, penciclovir) and uracil derivatives [e.g., 2′-fluoro-2′-deoxy-1-β-arabinofuranosyl-5-iodouracil (FIAU)]. In contrast, mammalian thymidine kinases phosphorylate acycloguanosines only minimally, making these substrates advantageous as reporter gene imaging probes (11). Acycloguanosine derivatives are currently used extensively both as cytotoxic pharmaceuticals to treat herpes infections and for HSV1-tk suicide gene therapy (13).

Improvements in sensitivity of the HSV1-tk reporter gene imaging assay can be achieved either by (i) identifying substrates that exhibit higher V_{max}/K_m for HSV1-TK or (ii) by engineering TK enzyme(s) with improved V_{max}/K_m for a particular reporter substrate. Decreased V_{max}/K_m of HSV1-TK for thymidine (an endogenous competitor) also should improve HSV1-tk reporter gene assay sensitivity. We previously demonstrated the advantages of using fluorine-18-labeled penciclovir, 8-[¹⁸F]fluoropenciclovir (FPCV), vs. 8-[¹⁸F]fluoroganciclovir (FGCV) as a reporter substrate for HSV1-TK (S.G., E.B., M.I., and M.N., unpublished work).

HSV1-tk mutants that more effectively utilize acycloguanosines as substrates are being sought to achieve greater toxicity in HSV1-tk suicide gene therapy (15). We reasoned that mutant HSV1-TK enzymes that exhibit greater cytotoxicity, presumably because of increased substrate V_{max}/K_m, also may serve as better reporter genes for *in vivo* imaging of gene expression, in combination with positron-labeled acycloguanosines. In this report, we describe results with a specific HSV1-tk mutant, HSV1-sr39tk (see Fig. 1). This variant was created by random sequence mutagenesis of HSV1-tk (15) and selected in *Escherichia coli* for the enhanced ability to convert

---

MEDICAL SCIENCES

the prodrugs acyclovir and/or ganciclovir into cytotoxic agents (unpublished data). C6 rat glioma cells stably transfected with HSV1-sr39tk demonstrate better accumulation (net uptake) of [³H]acycloguanosines and their fluorine-18 analogues in culture than do cells expressing HSV1-tk. MicroPET imaging, using FPCV, of mice bearing stably transformed tumors expressing HSV1-tk and HSV1-sr39tk demonstrate greater *in vivo* imaging sensitivity of the mutant HSV1-sr39tk PET reporter gene. When adenoviral vectors carrying these two genes are administered by means of the tail vein in mice, HSV1-sr39tk is a better PET reporter gene for imaging hepatic gene expression than is HSV1-tk.

Materials and Methods

Radiolabeled Compounds. [8-³H]Penciclovir ([8-³H]PCV) (17.6 Ci/mmol; 1 Ci = 37 GBq) and [8-³H]ganciclovir ([8-³H]GCV) (13.1 Ci/mmol) were obtained from Moravek Biochemicals (La Brea, CA). Radiochemical purity, determined by HPLC, was >97% for both compounds. FPCV and FGCV were synthesized as described (16), each with a specific activity of 2–5 Ci/mmol. Radiochemical purity of FGCV and FPCV exceeded 99%, as determined by HPLC.

Radioactivity Determinations. All tritium analyses were performed with a Beckman LS-6500 Liquid Scintillation Counter and Cytoscint (ICN) as scintillation fluid. Disintegrations per minute (dpm) were obtained by correcting for background activity and efficiency (69.3% for tritium) based on calibrated standards (Beckman). Tritium counts were also corrected for quenching effects. All fluorine-18 analyses were performed in either a dose calibrator (Capintec CRC-5R) or a well counter (Cobra II; Packard), correcting for efficiency differences between these two systems.

HPLC Analyses. [8-³H]GCV, [8-³H]PCV, FGCV, FPCV, and their metabolites from cell extracts were analyzed by using a Whatman Partisil 10 SAX column. The column was eluted with a linear KH₂PO₄ gradient, 0.01–1.0 M (pH 3.7, at a flow rate of 1 ml/min) and monitored with a UV detector wavelength set at 254 nm. Radioactive fractions were collected in samples taken over 1–2 min.

Construction and Purification of Adenoviruses. A replication-deficient adenovirus expressing the HSV1-sr39tk gene from a constitutive cytomegalovirus (CMV) promoter (Ad-CMV-HSV1-sr39tk) was constructed, purified, and characterized in the same way as previously described for the adenovirus expressing HSV1-tk (Ad-CMV-HSV1-tk) (17). An E1-deletion virus (17) was prepared for use as a control.

Cell Lines, Culture Conditions, and Transfection Procedures. C6 rat glioma cells (control cell line), the C6 HSV1-tk stable transfectant (C6-stb-tk+), and C6 HSV1-sr39tk stable transfectant (C6-stb-sr39tk+) were used. Expression vector, transductions, and selection of stable transfectants were as described in ref. 18. For [8-³H]GCV, FGCV, [8-³H]PCV, and FPCV uptake studies, cells were grown in 12-well plates, in DMEM supplemented with 5% FBS, 1% penicillin/streptomycin, and 1% L-glutamine.

For adenovirus infection studies, C6 cells were seeded as monolayers in T75 flasks. Twenty-four hours after plating, varying viral titers [0.1–0.50 × 10⁹ plaque-forming units (pfu)] of Ad-CMV-HSV1-sr39tk were added to the flasks, using the control virus to equalize the total viral titer among flasks at 0.50 × 10⁹ pfu. Cells were exposed to the adenovirus for 27 hr, then replated and cultured for an additional 22 hr in 12-well plates (for tracer uptake studies) or 100-mm dishes (for Northern blot analysis).

Western Blot Analysis. Cells and tumor tissues were lysed in a homogenization buffer containing pepstatin (1.45 mM), leupeptin (2.1 mM), DTT, triethanolamine (50 mM), and EDTA/EGTA (0.1 mM). Total protein (5–20 μg) was loaded in Laemmli buffer onto a 7.5% polyacrylamide stacking gel, run at 40 V, then at 100 V through a 7.5% separating gel by using a Mini Cell (Bio-Rad). The proteins were transferred to nitrocellulose membranes (Bio-Rad no. 162-0146) for 1 hr by using a Mini Trans-Blot Electrophoretic Transfer Cell (Bio-Rad). The membrane was then blocked in 1× PBS/0.05% Tween 20/5% nonfat dry milk overnight at 4°C. After two washes in 1× PBS/0.005% Tween 20, HSV1-TK polyclonal antiserum (15) was added for 1.5 hr. After another three washes, secondary antibody was added for 1.5 hr. Using the enhanced chemiluminescence (ECL) kit (Amersham Life Science no. RPN2106), the membrane was developed on Kodak film in the dark room. The film was then scanned for quantitation of the thymidine kinase signal. The membrane was then stripped and reprobed for β-actin by using the protocol described in the ECL kit. Total protein content loaded was then normalized by the β-actin signal.

Cell Uptake Studies. Uptake of [8-³H]GCV (0.76 μCi/ml, 1.5 × 10⁻⁵ mg/ml), FGCV (3 μCi/ml, 2.4 × 10⁻⁴ mg/ml), [8-³H]PCV (1.0 μCi/ml, 1.5 × 10⁻⁵ mg/ml), and FPCV (3 μCi/ml, 2.4 × 10⁻⁴ mg/ml) was directly compared in C6, C6-stb-tk+, and C6-stb-sr39tk+ cells. A higher concentration of FGCV and FPCV is required because of the lower specific activity of these compounds relative to [8-³H]GCV and [8-³H]PCV. Cells were incubated at 37°C for 15, 30, 60, 120, and 240 min. At the end of each incubation period, radioactivity in the medium was measured. The wells were washed with cold PBS, the cells were harvested by using a cell scraper, and the radioactivity in the cell pellet was determined. Triplicate samples were performed at each time point for all uptake studies. The same wells were also used to determine total protein content. Because the transfection efficiency of the tk gene in the C6-stb-tk+ and C6-stb-sr39tk+ cell lines may not be identical, results were normalized to relative TK protein (normalized to β-actin) present, as estimated from Western blots. Data are expressed as the net accumulation of probe in [dpm cells/(dpm of medium at start of exposure)/μg total protein/relative TK protein] ± SE. Incorporation of reporter probe into DNA was measured as described (4). Studies were also repeated with the extracellular concentrations of [8-³H]PCV and FPCV increased by a factor of 10.

Message Levels. Northern blot analyses were performed to determine the HSV1-tk and HSV1-sr39tk mRNA levels from cells and murine tumor extracts and normalized to glyceraldehyde-3-phosphate dehydrogenase (GAPDH) mRNA levels, as described (17).

PET Imaging of Mice. Animal care and euthanasia were performed with the approval of the University of California Animal Research Committee. Ten- to 12-week-old male nude mice (*nu/nu*, ≈28 g; Charles River Breeding Laboratories) were s.c. injected with ≈2 × 10⁷ C6 cells, C6-stb-tk+, and C6-stb-sr39tk+ cells. After 2–3 wk, tumor sizes varied between 5 and 10 mm and were large enough to be imaged. Separate mice were used to compare expression of HSV1-tk or HSV1-sr39tk in liver by tail-vein injection of mice with adenovirus 48 hr before microPET scanning. Mice were anesthetized by i.p. injection of ≈40 μl of a ketamine and xylazine (4:1) solution before the injection of tracer. Mice with tumors were placed in a spread prone position, while all other mice were placed in a supine position and scanned with the microPET. Acquisition time was 56 min (8 min per bed position, seven bed positions), and images were reconstructed by using filter-back projection and an iterative three-dimensional

base position	785	790	811
HSV1-tk	C T C A T C	T T C	G C C C T C
Amino Acid	L I	F	A L
HSV1-sr39tk	A T C T T C	C T C	T T C A T G
Amino Acid	I F	L	F M

Fig. 1. Sequence differences between HSV1-tk and HSV1-sr39tk. Point mutations in the nucleotide sequence are indicated in bold. Amino acids are shown below their three-base codons. HSV1-tk differs from HSV1-sr39tk by seven nucleotide substitutions leading to five different nonpolar amino acids.

reconstruction technique (19) with an isotropic image resolution of 1.8 mm and a volumetric resolution of ≈8 mm^3.

Quantitation of Fluorine-18 Retention in Murine Tumors/Liver by MicroPET Image Analysis. Regions of interest (ROI) were drawn over all tumor/liver images on decay-corrected coronal images. For ROIs placed over the liver, the left lobe of the liver was used. The counts per pixel per min obtained from the ROI were converted to counts per ml per min by using a calibration constant obtained from scanning a cylinder phantom in the microPET scanner. The ROI counts per ml per min were converted to counts per g per min, assuming a tissue density of 1 g/ml, and divided by the injected dose to obtain an image ROI-derived FPCV %ID/g.

Digital Whole-Body Autoradiography (DWBA). Freezing, preparation of mouse whole-body coronal sections (45 μm thickness), and DWBA were performed as described (17) by using a Fuji BAS 5000 PhosphorImager and digital plates with a resolution of ≈100 μm.

Results

[8-^{3}H]PCV and FPCV Accumulation Is Greater in C6 Cells Expressing the Mutant HSV1-sr39TK Enzyme Than in C6 Cells Expressing the Wild-Type HSV1-TK Enzyme. The mutant HSV1-sr39tk was identified as described (15). The seven point mutations, resulting in five amino acid changes, are shown in Fig. 1. We utilized a C6 glioma cell line stably transfected with a plasmid expressing the wild-type HSV1-tk gene (C6-stb-tk+) and a similar cell line stably transfected with a plasmid expressing the HSV1-tk mutant (C6-stb-sr39tk+) to compare the enzyme-dependent accumulation of both [8-^{3}H]PCV and FPCV. We first compared the level of expression of the TK proteins in C6-stb-tk+ and C6-stb-sr39tk+ cells. Five Western blot analyses were performed on total cellular protein to determine relative TK protein levels in each cell line (Fig. 2). Qualitatively, the HSV1-sr39TK band
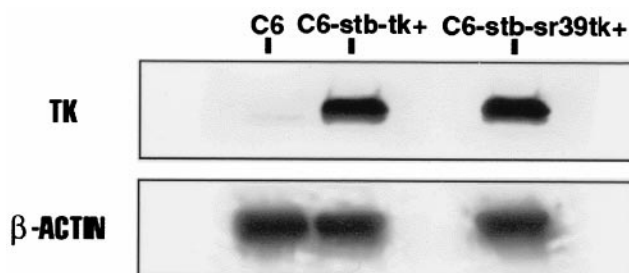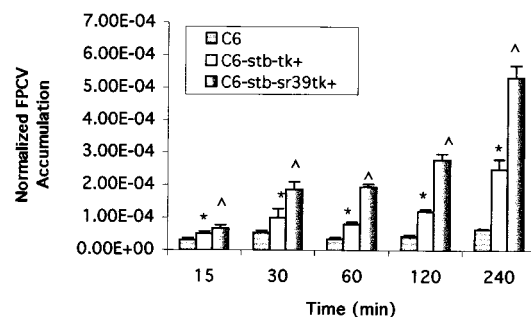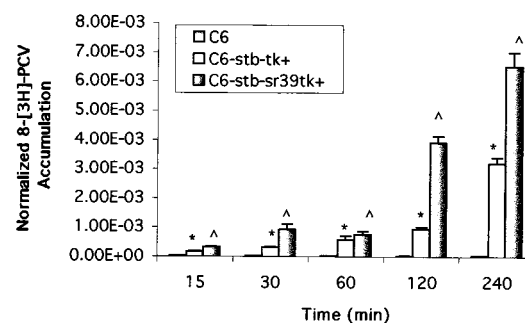
Fig. 3. [8-^{3}H]PCV and FPCV accumulation in stably transfected cells. The C6, C6-stb-tk+, and C6-stb-sr39tk+ cell lines were incubated with either [8-^{3}H]PCV (*Upper*) or FPCV (*Lower*) for the times shown. Values are net accumulation of each tracer (dpm cells/dpm medium at time zero), normalized both to μg of total protein and to relative TK levels as determined from a Western blot, as a function of time. The error bars represent the standard error for triplicate determinations. *, A significant difference ($P < 0.05$) compared to C6 control cells. ^, A significant difference ($P < 0.05$) compared to both C6 and C6-stb-tk+ cells.

from C6-stb-sr39tk+ cell extracts is similar in intensity to the HSV1-TK band from the C6-stb-tk+ cell extracts. A very faint band is visible from the C6 control cell extracts, presumably because of endogenous TK or a crossreacting protein. The Western blots were quantitated by using the computer program MACBAS (version 4.2, Fuji Photo Film). The five Western blots showed an average ratio [(TK/β-actin)/(sr39TK/β-actin)] of 1.4 ± 0.10. Data obtained in the cell tracer uptake studies (see below) were, therefore, corrected by a factor of 1.4 to normalize for total TK protein present.

There is a substantial difference ($P < 0.05$) in accumulation of [8-^{3}H]PCV between C6 control cells and both TK-expressing cell lines at all time points (Fig. 3 *Upper*). The C6-stb-sr39tk+ cell line accumulates more [8-^{3}H]PCV compared with the C6-stb-tk+ cell line at all time points ($P < 0.05$). We also observe higher levels of incorporation of FPCV in the C6-stb-sr39tk+ cell line, when compared with the C6-stb-tk+ cell line, at all time points >30 min (Fig. 3 *Lower*). We conclude from these data that uptake of both [8-^{3}H]PCV and FPCV resulting from expression of the reporter gene is significantly greater in C6 cells expressing HSV1-sr39TK than in C6 cells expressing HSV1-TK. No significant difference ($P < 0.05$) was observed in normalized tracer accumulation when utilizing [8-^{3}H]PCV, and FPCV concentrations increased 10-fold.

[8-^{3}H]GCV and FGCV Accumulation Is Also Greater in C6-stb-sr39tk+ Cells Than in C6-stb-tk+ Cells. Ganciclovir derivatives have previously been used to image HSV1-tk expression (4). Consequently, an additional experiment compared incorporation of [8-^{3}H]GCV and FGCV in C6, C6-stb-tk+, and C6-stb-sr39tk+ cells over time (data not shown). [8-^{3}H]GCV uptake in control C6 cells is significantly lower than uptake in the TK expressing

Fig. 2. Western blot of protein extracts from C6, C6-stb-tk+, and C6-stb-sr39tk+ cells. Staining with TK antiserum yields qualitatively similar signals for C6 cells expressing wild-type HSV1-tk (middle blot) and C6 cells expressing HSV1-sr39tk (right blot). Control C6 cells (left blot) show no significant signal. β-Actin expression is similar for all three cell lines. Total protein concentration used was 10 μg per lane for each cell type.

MEDICAL SCIENCES

cell lines ($P < 0.05$) at all time points. Significantly more [8-³H]GCV accumulation occurs in C6-stb-sr39tk+ cells than in C6-stb-tk+ cells ($P < 0.05$). Similarly, FGCV uptake in C6 cells is significantly lower than uptake in the TK-expressing cell lines ($P < 0.05$) and is significantly greater ($P < 0.05$) in the C6-stb-sr39tk+ cell line than in the C6-stb-tk+ cell line. [8-³H]PCV resulted in approximately 2-fold improved sensitivity compared with [8-³H]GCV in these experiments (data not shown), which is consistent with what we reported previously (S.G., E.B., M.I., and M.N., unpublished work). The expression of the HSV1-sr39TK enzyme results in greater retention of both FPCV and FGCV than does expression of the wild-type HSV1-TK enzyme.

C6-stb-sr39tk+ Cells Incubated with [8-³H]GCV, [8-³H]PCV, FGCV, and FPCV Produce Products Similar to Those Present in C6-stb-tk+ Cells. Metabolites from extracts of C6-stb-sr39tk+ and C6-stb-tk+ cells incubated with each of the four HSV1-TK substrates for 120 min have identical retention times. We observe four peaks at ≈3, 9, 16, and 32 min (data not shown). These results are consistent with previous results using C6-stb-tk+ cells (4) and reflect the peaks for each parent compound and its monophosphate, diphosphate, and triphosphate derivatives. Incorporation of the acycloguanosines into DNA also occurs, as previously reported for C6-stb-tk+ cells incubated with [8-³H]GCV and FGCV (4).

Ad-CMV-HSV1-sr39tk-Infected C6 Cells Accumulate FPCV in Proportion to Levels of HSV1-sr39tk Reporter Gene Expression. C6 cells were infected with varying titers ($0.1–0.5 \times 10^9$ pfu) of Ad-CMV-HSV1-sr39tk and additional control virus to maintain the total viral titer fixed to 0.5×10^9 pfu. Control and infected cells were incubated with [8-³H]PCV (1 μCi/ml) or FPCV (3 μCi/ml) for 120 min. Cells were harvested and assayed for (*i*) accumulation of radioactivity, and (*ii*) HSV1-sr39tk mRNA levels (normalized to GAPDH mRNA levels). C6 cells expressed increasing levels of GAPDH-normalized HSV1-sr39tk mRNA levels when infected with increasing levels of Ad-CMV-HSV1-sr39tk (Fig. 4 *Top*). We observe increasing accumulation of FPCV for cells infected with increasing levels of Ad-CMV-HSV1-sr39tk (Fig. 4 *Middle*). We also observe increasing levels of FPCV accumulation as a function of increasing HSV1-sr39tk mRNA (normalized to GAPDH) (Fig. 4 *Bottom*). Similar results were obtained for [8-³H]PCV incorporation, except that a larger dynamic range for accumulation of tritium radioactivity (range 3.6×10^{-4} to 7.0×10^{-3} normalized accumulation) was noted.

MicroPET and DWBA Imaging, Using FPCV as PET Reporter Probe, Is More Sensitive for HSV1-sr39tk as a Reporter Gene Than for HSV1-tk as a Reporter Gene. We first compared the sensitivity of HSV1-tk and HSV1-sr39tk *in vivo* by using tumor cells stably expressing these PET reporter genes. Three 12- to 14-wk-old nude mice were injected s.c. with ≈2×10^6 each of C6 cells, C6-stb-tk+ cells, and C6-stb-sr39tk+ cells. After 2–3 wk when tumor sizes varied between 0.5 and 1.0 cm, animals were scanned by using microPET. Because PET permits repeated imaging, all mice were imaged both with 2-[¹⁸F]fluoro-2-deoxyglucose (FDG) and FPCV. The FDG images of tumors can be directly compared with the image of reporter gene expression (Fig. 5). For FDG scans, mice were anesthetized and scanned 1 hr after tail vein injection of FDG (150–200 μCi). All tumors show FDG retention. Activity is also present in the urinary tract and the intestine, resulting from tracer clearance. High brain activity is also noted, reflecting the high glucose utilization in this organ. Twenty-four hours later, FPCV injection and microPET scans were performed as described for FDG. Mice were sacrificed immediately after the FPCV microPET scan and used for DWBA. For FPCV as a tracer, the greatest imaging signal is obtained from the HSV1-sr39tk-expressing tumor. A reduced signal is observed in
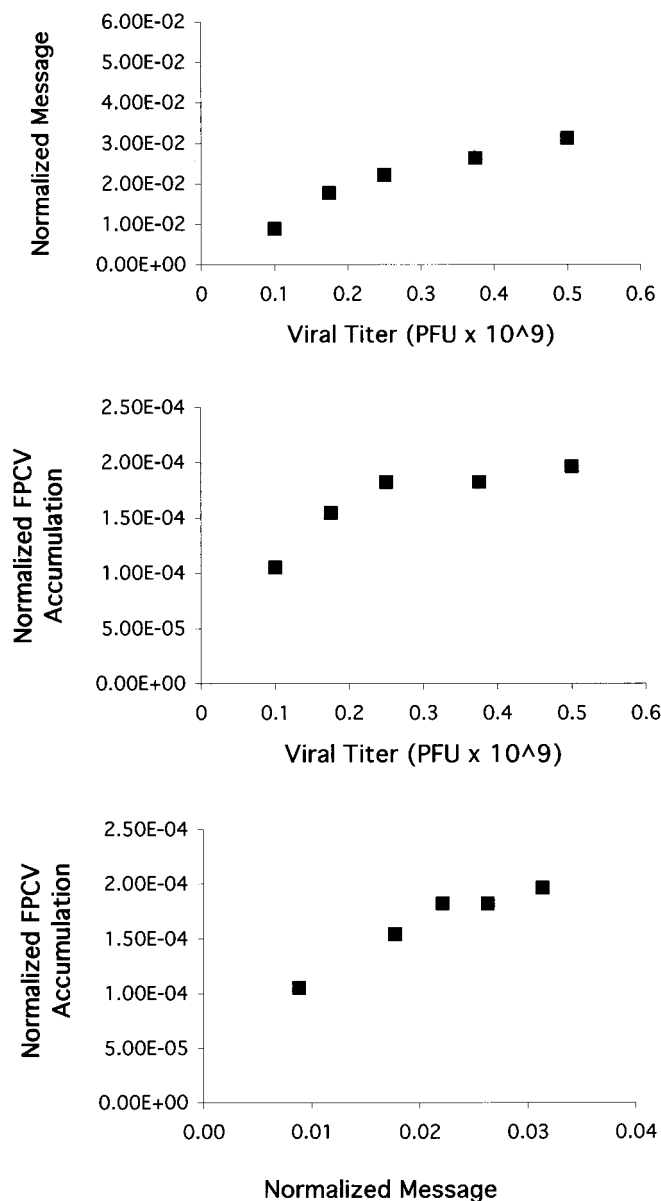

Fig. 4. FPCV accumulation in cells infected with Ad-CMV-HSV1-sr39tk. C6 cells were infected with five different viral titers of Ad-CMV-HSV1-sr39tk. Cells were subsequently exposed to FPCV for 120 min, then harvested and assayed for FPCV accumulation, HSV1-sr39tk mRNA, and GAPDH mRNA levels. (*Top*) HSV1-sr39tk mRNA levels (normalized to GAPDH levels) as a function of viral titer. (*Middle*) FPCV-normalized accumulation as a function of viral titer. The units of normalized FPCV accumulation are: [dpm cells/dpm medium at time zero/μg of total protein]. (*Bottom*) FPCV-normalized accumulation as a function of HSV1-sr39tk mRNA levels (normalized to GAPDH).

the tumor expressing HSV1-tk, and no significant signal is present in the control C6 tumor. The presence of TK protein in the C6-stb-tk+ and C6-stb-sr39tk+ tumor extracts was confirmed by Western blot analysis and showed near-identical levels (data not shown). TK expression normalized to β-actin was similar in the C6-stb-tk and C6-stb-sr39tk+ tumors [(TK/β-actin)/(sr39TK/β-actin), ≈1.0]. No TK expression was observed from the control C6 tumor extracts. In three mice, the relative retention of FPCV in C6-stb-sr39tk+ tumors as compared with C6-stb-tk+ tumors [%ID/g (sr39tk)/%ID/g (tk)] was 3.72 ± 0.30.
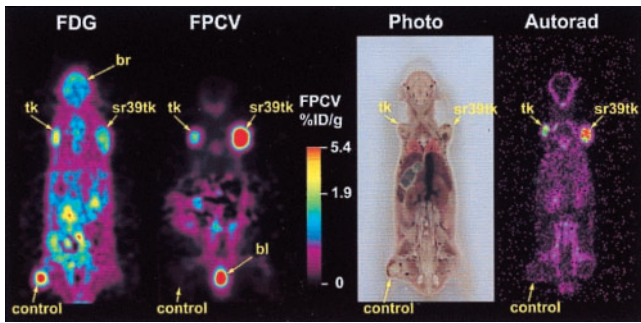
Fig. 5. FDG and FPCV MicroPET images and FPCV DWBA images of a mouse with C6, C6-stb-tk+, and C6-stb-sr39tk+ tumors. A nude mouse with three tumors was imaged with a microPET, first with FDG, and, 24 hr later, with FPCV. The mouse was sacrificed immediately after the FPCV scan and used for DWBA. A whole-body single-slice coronal projection image of fluorine-18 activity distribution for FDG is displayed on the left. The second panel shows a single-slice coronal projection image from the FPCV microPET image of the same mouse. The C6-stb-sr39tk+ tumor shows the strongest signal with FPCV. The C6-stb-tk+ tumor shows the next strongest signal, and the control C6 tumor shows minimal signal. The color scale represents the FPCV percent-injected dose per gram of tissue (%ID/g) (0.02% ID/g for the C6 control tumor, 1.9% ID/g for the C6-stb-tk+ tumor, and 5.3% ID/g for the C6-stb-sr39tk+ tumor). The third panel is a photograph of the coronal section used for DWBA (autorad). The fourth panel shows a DWBA obtained directly after the FPCV microPET scan. b, bladder; br, brain.

We also compared HSV1-tk and HSV-sr39tk *in vivo* imaging properties when these two genes are delivered by using an adenoviral vector. Tail vein injection of adenovirus carrying a reporter gene leads primarily to reporter gene expression in the liver (17). Swiss–Webster mice were tail-vein injected with 1×10^9 pfu of control virus (three mice), Ad-CMV-HSV1-tk virus (three mice), or Ad-CMV-HSV1-sr39tk virus (three mice). Forty-eight hours later, the mice were tail-vein injected with ≈ 150 μCi of FPCV (Fig. 6). After 60 min, the animals were imaged in a microPET scanner. FPCV retention is significantly greater ($P < 0.05$) in livers of mice injected with Ad-CMV-HSV1-sr39tk ($7.8 \pm 1.2\%$ ID/g liver) as compared with Ad-CMV-HSV1-tk ($3.4 \pm 0.8\%$ ID/g liver). The three mice injected with control virus showed significantly less activity ($P < 0.01$) than the mice injected with the other two viruses with a %ID/g
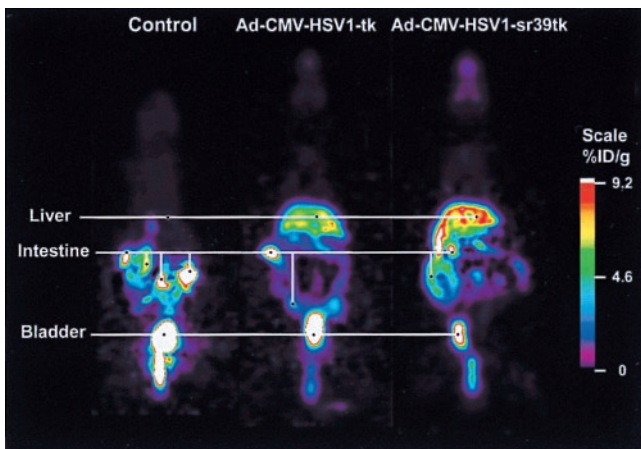

Fig. 6. MicroPET FPCV images of mice injected with control adenovirus, Ad-CMV-HSV1-tk, or Ad-CMV-HSV1-sr39tk. FPCV coronal microPET images from a mouse injected with control virus (*Left*), Ad-CMV-HSV1-tk virus (*Middle*), and Ad-CMV-HSV1-sr39tk virus (*Right*). Each viral vector (1.0×10^9 pfu) was injected 48 hr before injection of FPCV. The microPET images were obtained 1 hr after the injection of FPCV.

liver of 0.2 ± 0.1. Background activity in kidneys, bladder, and gastrointestinal tract was observed in all mice, resulting from clearance of FPCV from these routes.

Discussion

Our initial development of the HSV1-tk PET reporter gene system used wild-type HSV1-tk enzyme as the PET reporter gene and FGCV as the PET reporter probe (4, 17). In our original studies, the HSV1-tk/FGCV *in vivo* imaging system was less sensitive when compared with our other PET reporter gene/PET reporter probe system [the D2R and 3-(2'-[18F]fluoroethyl)spiperone (FESP) (6)]. We recently described an improvement in sensitivity of HSV1-tk imaging by using FPCV as a reporter probe (S.G., E.B., M.I., and M.N., unpublished work) and now demonstrate further enhanced sensitivity by using HSV1-sr39tk.

HSV1-sr39TK is clearly able to utilize acycloguanosines more effectively than HSV1-TK. In C6 cells stably transformed with these two genes, both in cell culture and in tumors, HSV1-sr39TK more effectively sequesters [8-³H]GCV, [8-³H]PCV, FGCV, and FPCV than does wild-type HSV1-TK. The same increased ability of the mutant HSV1-sr39TK enzyme to trap acycloguanosine derivatives, relative to the wild-type HSV1-TK enzyme, is evident when the two PET reporter genes are delivered by means of an adenovirus delivery system to mice *in vivo*. For increasing titers of Ad-CMV-HSV1-sr39tk, greater accumulation of tritiated and fluorinated acycloguanosines occurs both in cultured cells and mice. In culture and *in vivo*, the sequestration of acycloguanosine imaging probes is greater, per unit of TK protein expressed, for mutant HSV1-sr39tk than for wild-type HSV1-tk.

Studies to verify changes in K_m and/or V_{max} for the various substrates and the two enzymes (HSV1-sr39TK and HSV1-TK) should help to further clarify the advantages of the mutant enzyme. The observed differences in culture and *in vivo* are likely because of a better V_{max}/K_m ratio for FPCV and HSV1-sr39TK vs. FPCV and HSV1-TK. Furthermore, the relative gain in sensitivity when utilizing HSV1-sr39TK does not depend on specific activity, as the normalized accumulation in cell culture did not depend on extracellular concentration of each reporter probe over the range tested. It is also unlikely that the observed differences between the two enzymes are because of changes in levels of nucleoside transporter in cells or tissues expressing HSV1-TK vs. HSV1-sr39TK, since otherwise identical cell lines were used for culture experiments, and otherwise identical delivery vehicles and target tissues were used for *in vivo* studies. Tracer kinetic studies utilizing dynamic PET data should help to quantitate and distinguish the cell uptake and phosphorylation processes.

A number of positron-labeled substrates have now been developed for *in vivo* imaging of the HSV1-tk PET reporter gene. These include FGCV, FPCV, [124I]FIAU (reviewed in ref. 11) and FHBG (penciclovir fluorinated on the side chain, rather than at the 8-carbon position; ref. 21). Each of these HSV1-TK PET reporter probes has its advantages and disadvantages; variables include ease of synthesis, specific activity, V_{max}/K_m for the HSV1-TK reporter enzyme, *in vivo* stability, and blood and tissue clearance times. We are currently exploring the use of FHBG as an alternative substrate for both the wild-type HSV1-TK and mutant HSV1-sr39TK PET reporter enzymes. We are also comparing FIAU to FHBG and FPCV in cell culture and *in vivo*.

It is fortunate that PCV and FPCV are better substrates for HSV1-sr39tk than for HSV1-tk, since the HSV1-sr39TK mutant enzyme was isolated by using a screening protocol designed to identify HSV1-TK enzymes more effective with ganciclovir (15). However, [8-³H]PCV is more effectively accumulated than is FPCV in cells that express either HSV1-tk or HSV1-sr39tk. The

greater effectiveness of [8-³H]PCV as substrate may be because of the electronegative character of the fluorine at position C8 of FPCV. The presence of a fluorine atom in FPCV could perturb the electron density in the imidazole ring, causing a reduction in the efficiency of FPCV binding to the HSV1-TK enzyme pocket, which depends mainly on hydrogen bonding (14). In addition, FPCV and [8-³H]PCV may have different uptake characteristics.

It should be possible to increase the efficacy of the HSV1-tk PET reporter gene system even more by applying mutagenesis schemes similar to that used to isolate HSV1-sr39tk to the HSV1-tk gene and by using FPCV (for example) as a screening compound in cytotoxicity assays. FPCV is incorporated into DNA of cells expressing HSV1-tk and HSV1-sr39tk (S.S.G., E.B., and M.I., unpublished observations) and should—like the other acycloguanosines—result in chain termination and/or inhibition of the polymerase. By screening for HSV1-TK enzyme mutants that show greater relative cell toxicity with FPCV, it should be possible to identify mutant HSV1-tk PET reporter genes that give even greater sensitivity for imaging than does HSV1-sr39tk.

The HSV1-sr39tk/FPCV and D2R/FESP PET reporter gene/ PET reporter probe *in vivo* gene imaging systems now have essentially equivalent sensitivities. The major applications of *in vivo* gene imaging with PET reporter genes are likely to be (*i*) repetitive and quantitative monitoring of the location, magnitude, and duration of gene expression from gene therapy vehicles and (*ii*) the repetitive and quantitative evaluation of reporter gene expression in transgenic animals. The two PET reporter gene systems, HSV1-sr39tk/FPCV and D2R/FESP, have distinct advantages and disadvantages. (*i*) The wild-type HSV1-tk gene is used with pharmacologic levels of acycloguanosines in a number of conventional cell suicide protocols, both in constructing experimental animal models and in current gene therapy approaches. Thus, current applications exist for this imaging system. The HSV1-sr39tk mutant, with its increased cytotoxicity after acycloguanosine administration in pharmacologic amounts, is likely to be incorporated into such protocols. In contrast, the D2R gene has no applications of this nature. (*ii*)

Expression of the HSV1-TK enzymes, in the absence of exogenous acycloguanosine substrates, has little or no effect on cells and tissues. In contrast, it is possible that ectopic expression of the wild-type D2R gene, either in transgenic animals or in bicistronic gene therapy delivery vehicles, might have physiological consequences as a result of interactions with endogenous ligands. (*iii*) On the other hand, the substrates for HSV1-tk reporter genes do not cross the blood–brain barrier (in contrast to FESP), thus preventing the easy utilization of the HSV1-tk PET reporter gene systems for *in vivo* imaging of the brain in the presence of an intact blood–brain barrier. (*iv*) In addition, male animals carrying HSV1-tk transgenes are frequently sterile, as a result of a cryptic transcription start site for enzyme expression that functions in the testes (20). (*v*) Finally, chronic expression of the HSV1-tk gene after somatic transfer, as occurs in gene therapy protocols, results in an immune response to the protein that may lead to unintended consequences. We, and other laboratories, are modifying these reporter systems to overcome some of these limitations.

There are many experimental situations in which availability of two *in vivo* reporter genes will be of considerable utility. Thus, for example, if one wants to track the location, proliferation, and viability of both a tumor cell population and immunologically responsive cells that migrate to the tumor in the same animal, it is now possible to identify each of these cell populations individually, if each cell population expresses a different PET reporter gene. Similarly, our ability to image two distinct reporter genes *in vivo* will allow direct comparisons, in the same individual, of alternative gene delivery vehicles in somatic gene transfer protocols.

1. Contag, P. R., Olomu, I. N., Stevenson, D. K. & Contag, C. H. (1998) *Nat. Med.* **4,** 245–247.
2. Tjuvajev, J. G., Finn, R., Watanabe, K., Joshi, R., Oku, T., Kennedy, J., Beattie, B., Koutcher, J., Larson, S. & Blasberg, R. G. (1996) *Cancer Res.* **56,** 4087–4095.
3. Bogdanov, A. & Weissleder, R. (1998) *Trends Biotechnol.* **16,** 5–10.
4. Gambhir, S. S., Barrio, J. R., Phelps, M. E., Iyer, M., Namavari, M., Satyamurthy, N., Wu, L., Green, L. A., Bauer, E., MacLaren, D. C., *et al.* (1999) *Proc. Natl. Acad. Sci. USA* **96,** 2333–2338.
5. Tjuvajev, J. G., Avril, N., Oku, T., Sasajima, T., Miyagawa, T., Joshi, R., Safer, M., Beattie, B., DiResta, G., Daghighian, F., *et al.* (1998) *Cancer Res.* **58,** 4333–4341.
6. MacLaren, D. C., Gambhir, S. S., Satyamurthy, N., Barrio, J. R., Sharfstein, S., Toyokuni, T., Wu, L., Berk, A. J., Cherry, S. R., Phelps, M. E. & Herschman, H. R. (1999) *Gene Ther.* **6,** 785–791.
7. Gambhir, S. S., Barrio, J. R., Herschman, H. R. & Phelps, M. E. (1999) *J. Nucl. Cardiol.* **6,** 219–233.
8. Phelps, M. E., Hoffman, E. J., Mullani, N. A. & Ter-Pogossian, M. M. (1975) *J. Nucl. Med.* **16,** 210–224.
9. Phelps, M. E. (1991) *Neurochem. Res.* **16,** 929–994.
10. Yu, Y., Alexander, J. A., Barrio, J. R., Toyokuni, T., Satyamurthy, N., Namavari, M., Cherry, S. R., Phelps, M. E., Herschman, H. R. & Gambhir, S. S. (2000) *Nat. Med.*, in press.

11. Gambhir, S. S., Barrio, J. R., Herschman, H. R. & Phelps, M. E. (1999) *Nucl. Med. Biol.* **26,** 481–490.
12. Cherry, S. R., Shao, Y., Silverman, R. W., Meadors, K., Siegel, S., Chatziioannou, A., Young, J. W., Jones, W. F., Moyers, J. C., Newport, D., *et al.* (1997) *IEEE Trans. Nucl. Sci.* **44,** 1161–1166.
13. Moolten, F. L. (1997) *Sci. Med.* **4,** 16–25.
14. Brown, D. G., Visse, R., Sandhu, G., Davies, A., Rizkallah, P. J., Melitz, C., Summers, W. C. & Sanderson, M. R. (1995) *Nat. Struct. Biol.* **2,** 876–881.
15. Black, M. E., Newcomb, T. G., Wilson, H.-M. P. & Loeb, L. A. (1996) *Proc. Natl. Acad. Sci. USA* **93,** 3525–3529.
16. Namavari, M., Barrio, J. R., Gambir, S. S., Cherry, S. R., Herschman, H. R., Phelps, M. E. & Satyamurthy, N. (2000) *Nucl. Med. Biol.*, in press.
17. Gambhir, S. S., Barrio, J., Wu, L., Iyer, M., Namavari, M., Satyamurthy, N., Bauer, E., Parrish, C., MacLaren, D., Borghei, A., *et al.* (1998) *J. Nucl. Med.* **39,** 2003–2011.
18. Kokoris, M. S., Sabo, P., Adman, E. T. & Black, M. E. (1999) *Gene Ther.* **6,** 1415–1426.
19. Qi, J., Leahy, R. M., Cherry, S. R., Chatziioannou, A. & Farquhar, T. H. (1998) *Phys. Med. Biol.* **43,** 1001–1013.
20. Ellison, A. R., Wallace, H., al-Shawi, R. & Bishop, J. O. (1995) *Mol. Reprod. Dev.* **41,** 425–434.
21. Alauddin, M. M. & Conti, P. S. (1998) *Nucl. Med. Biol.* **25,** 175–180.